CALIBRATION AND TESTING OF A LARGE-SCALE ELECTRIC GUN FOR SHOCK HUGONIOT MEASUREMENTS

AR-008-293

DAVID J. HATT AND PHILIP F.X. RYAN

MRL-TR-93-24

OCTOBER 1993

(2)

MATERIALS RESEARCH LABORATORY

DSTO

Calibration and Testing of a Large-Scale Electric Gun for Shock Hugoniot Measurements

David J. Hatt and Philip F.X. Ryan

MRL Technical Report
MRL-TR-93-24

Abstract

This report presents further work on the MRL large-scale electric gun facility including the use of a screened room and a purpose-built safety interlock system, calibration of an electric gun using a VISAR velocity interferometer, and tests on two laser break-beam arrangements for measuring flyer velocity. The VISAR was also used for making velocity measurements during some impact experiments on several materials to test the suitability of the facility for obtaining Hugoniot and spall strength data. The materials were Perspex and Lexan (polymethyl methacrylate and polycarbonate) and aluminium alloy 3105.

The flyer velocities measured using the break-beam arrangements were compared with those measured by the VISAR. The agreement between the two methods was found to be poor and inconsistent. High-speed photographs show leakage of plasma past the flyer. Interruption of the laser beams by the plasma instead of the flyer seems to be the reason for the poor agreement. The Hugoniot and spall strength data were in general agreement with published data.

DEPARTMENT OF DEFENCE
DSTO MATERIALS RESEARCH LABORATORY

Published by

DSTO Materials Research Laboratory
Cordite Avenue, Maribyrnong
Victoria, 3032 Australia

Telephone: (03) 246 8111
Fax: (03) 246 8999

AR No. 008-293

APPROVED FOR PUBLIC RELEASE

Authors

David J. Hatt

David Hatt graduated Dip App Physics from the Ballarat School of Mines and Industries in 1968, and joined MRL in 1969. Until transferring to the Explosives Ordnance Division in 1977, he worked on Defence standards and calibration systems. In the Explosives Ordnance Division he has specialized in the development and application of instrumentation for the study of high-speed events and phenomena related to explosives and ammunition.

Philip F.X. Ryan

Philip Ryan was sponsored by MRL's Explosives Ordnance Division as a Cadet Research Scientist from 1988 to 1992. His doctoral thesis ("The production and measurement of shock waves in solid materials") with the Australian National University's Department of Physics was submitted in 1992. In 1987 he was awarded a BSc (Hons, first class) in Physics by the University of Melbourne. Philip is now in Ship Structures and Materials Division, working on radar signature management.

Contents

Calibration and Testing of a Large-Scale Electric Gun for Shock Hugoniot Measurements

1. Introduction

Research in the area of explosives effects (e.g., initiation and detonation phenomena, and explosive/target interaction) invariably requires a knowledge of the behaviour of materials, both inert and reactive, when subjected to shock waves. Predictions made using simple shock-impedance matching calculations or, for more complex configurations, wave propagation computer codes use in both cases the known Hugoniot data for the materials of interest. These Hugoniot data have been typically obtained from impact experiments where plane shock wave conditions have been generated by flying plates driven by explosives, exploding bridge foils, or compressed gas [1].

In recent years, the Explosives Ordnance Division of MRL has had a requirement to develop its own capability for obtaining Hugoniot data. The quickest and cheapest way to do this was to construct an electric gun facility, though the data were expected to be less accurate than that that could be obtained from a gas gun facility [2]. The electric gun facility could also be adapted for investigating initiation properties of reactive materials, viz., run-to-detonation and failure diameter data, and pressure-duration effects (e.g. Walker-Wasley criterion [3]).

The initial development of this facility involved the design and experimental characterization of two electric guns called Boomer I and Boomer II [4]. The present report describes further development of the facility including the use of a screened room and a purpose-built safety interlock system, calibration of one of the electric guns using a VISAR velocity interferometer [5], and tests on two laser break-beam arrangements for measuring flyer velocity. The report also describes some shock impact experiments on several materials to test the suitability of the facility for obtaining Hugoniot and spall strength data. The experimental technique for obtaining the Hugoniot data is that described in detail in Podlesak's *et al.* report [4]. Briefly, the shock Hugoniot of most materials is given by the empirical relationship

$$U_s = c_o + su_p \qquad (1)$$

where U_s and u_p are the shock and particle velocities, respectively, c_0 is the nominal sound velocity in the unshocked material, and s is a constant. Hence, the measurement of U_s and u_p is sufficient to obtain the Hugoniot in shock velocity-particle velocity variables. Materials which do not follow (1) can usually be modelled by higher-order polynominials [6]. Most metals are linear while most plastics are second- or third-order.

2. *Experimental*

2.1 *Electric Gun Arrangement*

The electric gun arrangement is shown in the schematic diagram in Figure 1 and is essentially the Boomer II device [4]. Circuit currents were measured by means of a Rogowski coil installed around the earthed capacitor terminal. A 1 GΩ 1000:1 HV dc-probe was used for measuring the capacitor charge voltage. For synchronization purposes, a micro-switch operated by movement of a pneumatic plunger provided a trigger pulse via a capacitor discharge circuit. From ringdown tests [4] (performed with the transmission line shorted) the circuit inductance and resistance were found to be approximately 160 nH and 8 mΩ, respectively.

2.2 *Electric Gun Facility*

2.2.1 *Screened Room*

Operation of the electric gun presents electromagnetic interference (EMI) problems for electronic instrumentation and components; this was particularly so for the photomultiplier tubes (PMTs) used in the VISAR velocity interferometer. In addition, as the gun was located in an explosives building, a safety study [7] was undertaken which showed that its operation without suitable shielding would be an RF hazard for some types of electro-explosive devices that could be in the building. To obviate both of these problems the gun was enclosed by a screened room (Fig.2) which employed the principle of double electrical isolation [8]. The fully demountable, timber framed sides of the room were faced on both sides with brass mesh.

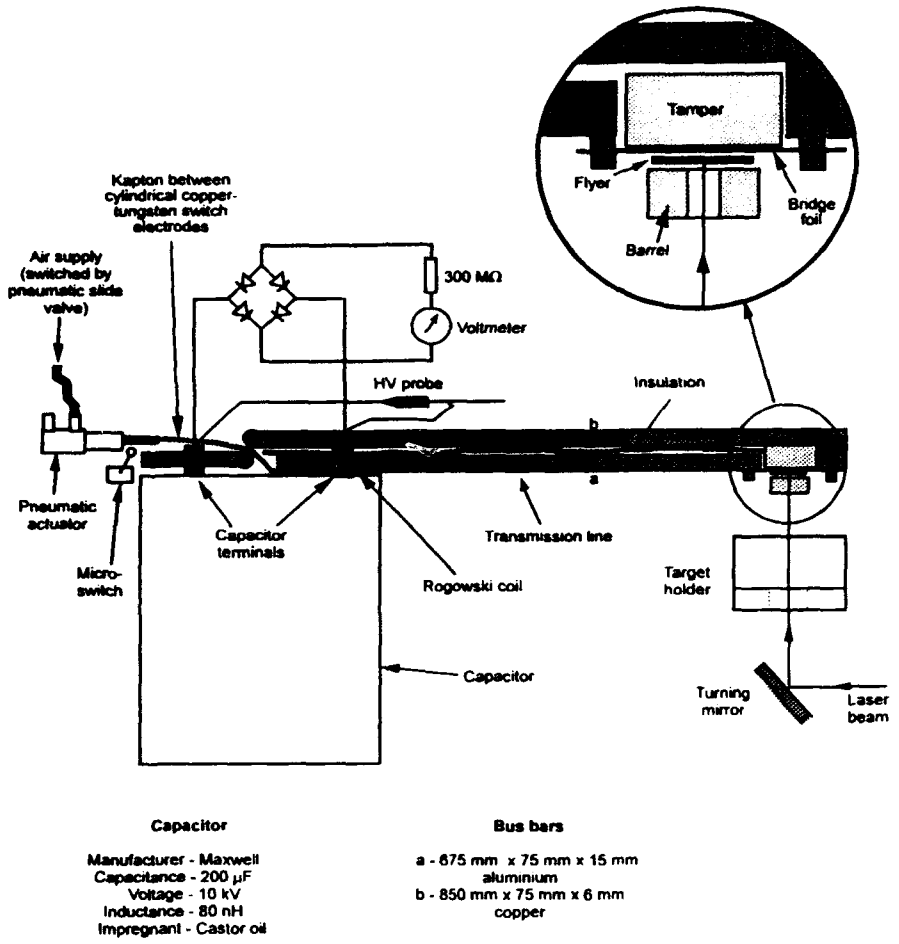

Figure 1: The electric gun arrangement.

RFI power line filters were mounted at one end of the room next to the safety earth. When using such filters, a low impedance earth connection is essential to avoid the possibility of the room reaching unsafe voltages due to leakage currents [9]. The safety earth comprised a 150 x 1 x 2000 mm^3 solid copper strap connecting the room to a 2 m length of copper tubing (Fig.2). After burial to its full length, the tube was filled from the top with $CuSO_4$ crystals. Holes drilled in the tube allow the $CuSO_4$ to leach into the surrounding soil to improve the integrity of the tube/soil contact [10]. The inner and outer shields of the room had a single point connection to the safety earth. The cable feedthrough panel was connected to the inner shield only. The VISAR laser beam entered the room through two circular metallic waveguides one each attached to the inner and outer shields as shown in Figures 2 and 18. The dimensions of each waveguide (90 mm diameter and 150 mm length) were selected for 100 dB attenuation at frequencies below 500 MHz using the expression [11]

$$\gamma = \frac{54.6}{\lambda_c}\sqrt{1-\left(\frac{\lambda_c}{\lambda}\right)^2} \qquad (2)$$

where γ = attenuation in dB/unit length, λ = free space wavelength, and λ_C = cutoff wavelength of the guide.

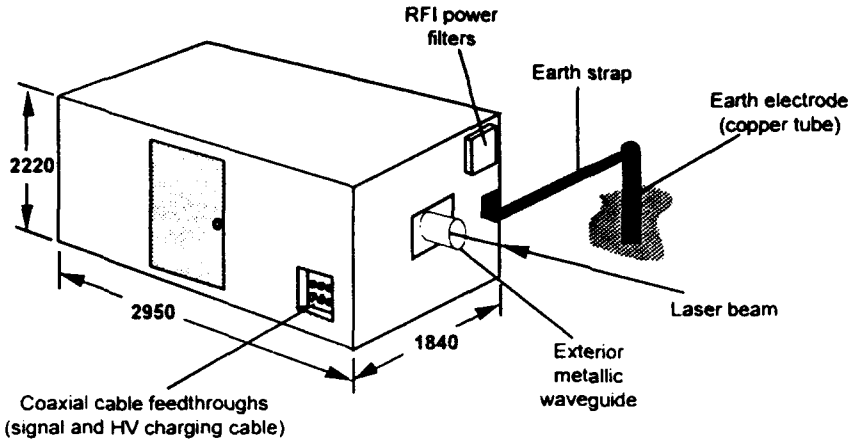

Figure 2: Exterior view of the screened room.

2.2.2 *Safety Interlock System*

A purpose-built Safety Interlock System (SIS) was installed in the facility to ensure that personnel would be safe during operation of the electric gun. The SIS comprised a Voltage Switching Unit (VSU), a Remote Control Panel (RCP), and an Interlock Patch Panel (IPP). The RCP and IPP were located in an adjoining room to the facility (Fig.3).

The VSU was connected to single- and three-phase mains outlets. Two electrical contactors in the VSU switched the mains to outlets on the VSU but only when an umbilical cord connected the VSU to the RCP. Several single-phase VSU outlets were used for instrumentation while a single three-phase VSU outlet was used for the VISAR's argon-ion laser. Two additional contactors in the VSU switched power to interlocked outlets (one single-phase and one three-phase). The three-phase interlocked outlet provided power to the HV power supply for charging the capacitor. The interlock contactors required seven sense switches to be closed before they could be actuated. Sense switches were installed on the doors to the gun facility, the door to the screened room, the capacitor pull-switch, the walls within the facility, and in a warning system unit (flashing lights and siren). The wall-mounted switches were latching switches and provided for emergency shut-down of the HV equipment. A key release latching switch on the RCP could be used for shutting-down the complete system.

The SIS had a fail-safe configuration where the capacitor was connected in series with a dump resistor in the VSU. With all sense switches closed, turning a key switch on the RCP operated the interlock contactors. On pressing the charge button on the RCP, HV vacuum relays in the VSU connected the capacitor to the HV power supply, enabling the capacitor to be charged. When the required charge voltage had been attained, the isolate button on the RCP was pressed to isolate the capacitor from the HV power supply. The pneumatically operated pull-switch was then actuated to discharge the capacitor through the transmission line. The sense switch on the pull-switch then opened, causing the interlock contactors in the VSU to open, removing mains power from the HV power supply, and returning the capacitor to the fail-safe configuration. In the event the capacitor failed to discharge, or the test needed to be aborted, turning the key switch on the RCP also returned the VSU to the fail-safe configuration.

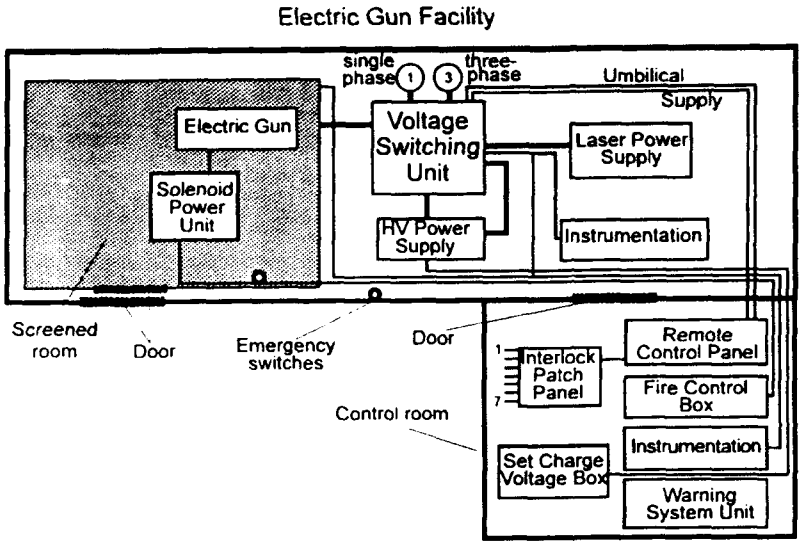

Figure 3: The electric gun facility and control room.

2.3 *Velocity Measurements*

2.3.1 *Flyer Velocity*

Relationships between peak flyer velocity and capacitor charge voltage (firing voltage) were required for use as calibration curves. The peak flyer velocities were obtained from continuous velocity-time histories measured by means of the VISAR velocity interferometer system shown in Figure 4. The nominal firing voltage range was 3.0 kV to 7.5 kV.

Several problems were encountered. The velocity measurements needed to be performed over long flight distances (> 20 mm), there was a large amount of self-light from the hot plasma produced on bridge burst, and, as switching of the electric gun was not performed electrically, no ready means for synchronization of PMT operation to bridge burst was available.

A 200 mm diameter lens with a focal length of approximately 1150 mm was used to focus the laser beam on to the target and for the collection of reflected light from the target. With this lens, intensity changes caused by target movement of > 20 mm were not excessive. The beam reducing telescope usually used with the VISAR [5] was not needed. The turning mirror (aluminium front coated) was protected by ≈ 10 mm thick Perspex (polymethyl methacrylate) positioned at a stand-off distance of 50 mm to 100 mm from the launch position. The target-to-lens distance was approximately 1.53 m while the lens-to-VISAR distance was approximately 3.4 m.

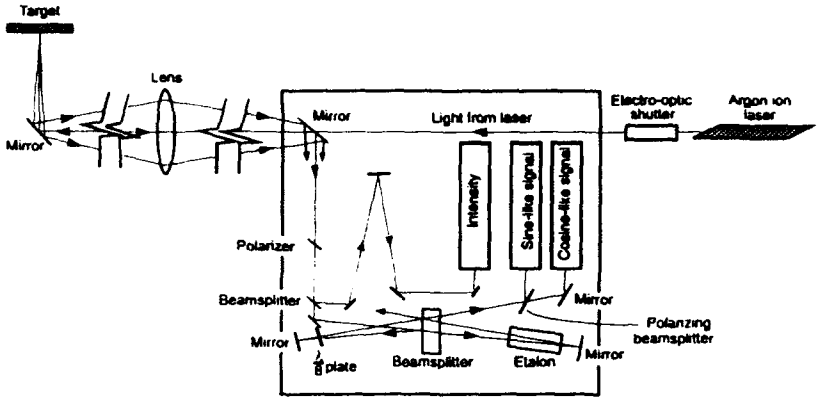

Figure 4: The MRL VISAR system as used with the electric gun.

The self-light was filtered by the laser line filters in front of the PMTs [5]. However, velocity measurements with the laser beam reflected directly from the flyer surface (grit blasted) were unsuccessful because the signals from the laser light returned to the VISAR were found to be low compared to the signals from the self-light and EMI. The laser was operated at its highest power (≈ 0.8 W) during these tests. It was subsequently found that successful measurements could be made by fixing self-adhesive retroreflective tape (No. 7615 Scotchlite, approximately 0.12 mm thick) to the flyer surface. The tape attenuated the self-light to a low level while increasing the level of reflected laser light, thereby improving the signal-to-noise ratio.

The PMTs are operated in pulse mode [5] and normally provide an experiment time of about 0.1 ms. Triggering of the PMTS from the Rogowski coil signal was attempted but found to be an unsuitable method because of an excessive delay in the PMT trigger circuitry. It was also found that the trigger circuitry could not be readily converted for continuous mode operation of the PMTs. Synchronization was achieved by increasing the experiment time of the PMTs to about 1 ms (by increasing the discharge time constant of the trigger circuit) and using the trigger pulse from the event circuit initiated by the micro-switch on the pneumatic plunger (Fig.1).

Aluminium bridge foils [4] with bridge dimensions of approximately 15 mm length and 10 mm width were used. Two bridge foil thicknesses were tested. The first series of tests were performed with a bridge foil thickness of 15 μm but these

were found to produce low peak velocities. For the subsequent tests, the bridge foil thickness was 35 μm.

To assemble the exploding bridge foil, the foil was firstly bonded to a Perspex or Lexan (polycarbonate) tamper (Fig.5). A piece of Lexan of 0.47 mm thickness was then fixed over the bridge foil to which the retroreflective tape was then attached. Lastly, Perspex or Lexan barrels, generally of 9 mm length and 11.5 mm diameter, were attached using double-sided adhesive tape. (Several tests were performed with different barrel lengths or diameters.) Except for the retroreflective tape and the barrels, the components of the assembly were bonded by means of cyanoacrylate adhesive.

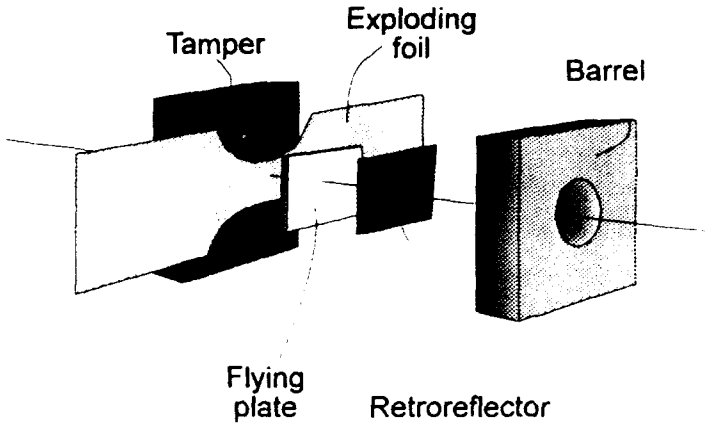

Figure 5: The exploding bridge foil assembly with tamper, Lexan flyer, retroreflector, and barrel.

The Rogowski coil signal was attenuated by means of a purpose-built voltage divider (Fig.6). Current-time histories through the coil were calculated from

$$i = \int_0^t \frac{\alpha V_A}{s} dt \qquad (3)$$

where V_A = voltage divider output voltage, α = voltage divider attenuation factor ≈ 400, and s = coil sensitivity = 22.4 nH [4].

For some tests, the Rogowski coil was used with a passive integrator circuit (Fig.7). Current-time histories were then calculated using

$$i = \frac{\tau}{s} V_R \qquad (4)$$
$$= 10^4 V_R \quad (C_{cable} \approx 2.4 \text{ nF})$$

where τ = time constant of the integrator = 224 μs, and V_R = integrator output voltage.

A typical instrumentation arrangement is shown in Figure 8.

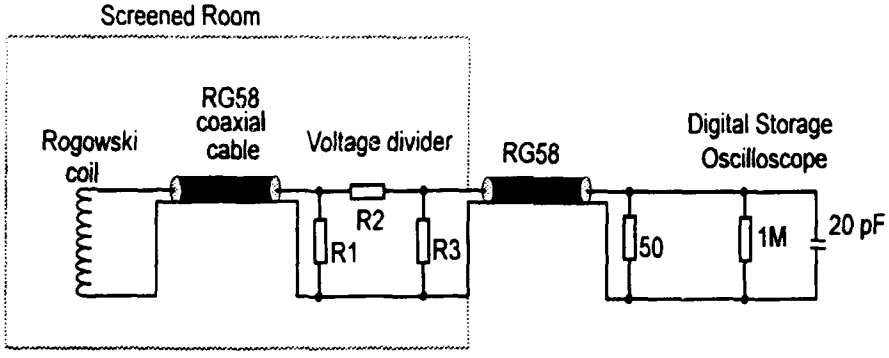

415:1 Voltage Divider:

R1 = 5 x 10 Ω (series) = 50 Ω
R2 = 10 x 1 kΩ (series) = 10 kΩ
R3 = 10 x 470 Ω (parallel) = 47 Ω

40:1 Voltage Divider:

R1 = 5 x 10 Ω (series) = 50 Ω
R2 = 2 x 470 Ω (series) = 940 Ω
R3 = 10 x 470 Ω (parallel) = 47 Ω

Figure 6: Pulse current measurement arrangement using a Rogowski coil and voltage divider.

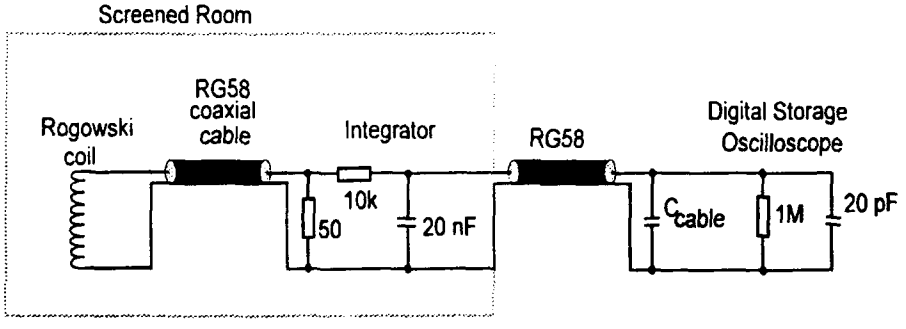

Figure 7: Pulse current measurement arrangement using a Rogowski coil and passive integrator.

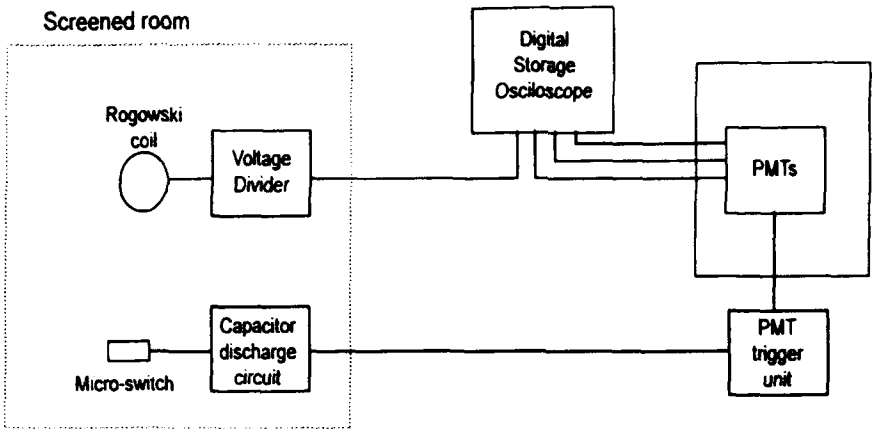

Figure 8: *Block diagram of the instrumentation arrangement for the electric gun calibration and laser break-beam tests.*

2.3.2 *Laser Break-Beam and Time-of-Arrival Methods*

For many impact experiments it would not be possible to measure the flyer velocity using the VISAR. This would occur, for example, when the target material is opaque or, for transparent targets, when a retroreflective or suitably reflective coating cannot be placed on the flyer. Thus use of an alternative method, such as a break-wire and break-beam arrangement [4], would need to be considered. Tests were conducted to evaluate two different laser break-beam arrangements of interest.

The first arrangement (Fig.9) used a single 10 mW He-Ne laser beam to provide an average velocity calculated from the transit time for the flyer to travel from the launch postion to the beam position. To obtain an estimate of the peak flyer velocity, the second arrangement (Fig.10) comprised two closely spaced beams positioned about 1 mm in front of the barrel exit. A laser line filter was required in both arrangements to remove self-light collected from the bridge burst. For some tests, a time-of-arrival (TOA) arrangement (Fig.11) was used concurrently with the dual break-beam arrangement. Simultaneous velocity measurements were made using the VISAR.

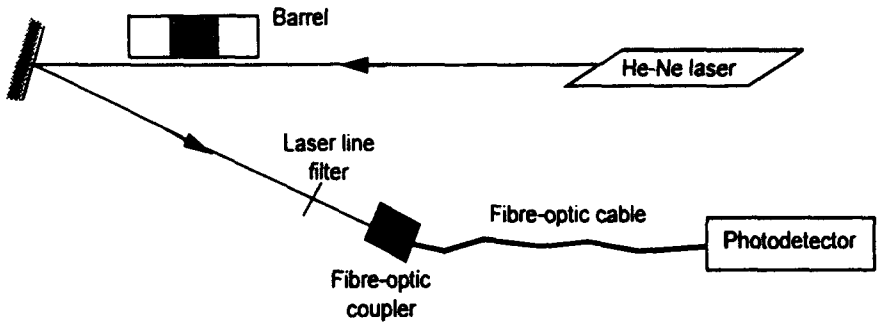

Figure 9: Single break-beam arrangement.

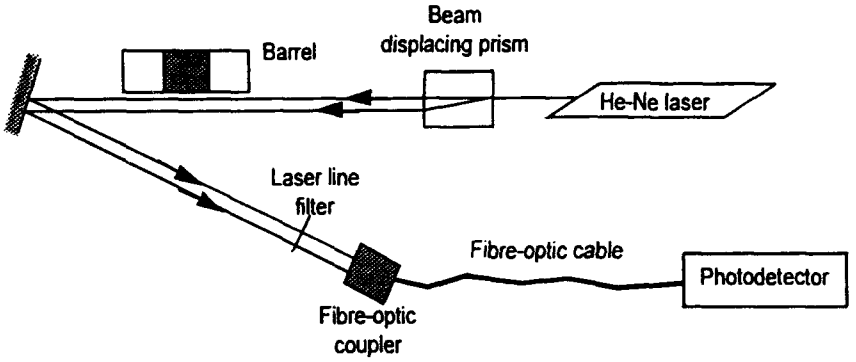

Figure 10: Dual break-beam arrangement.

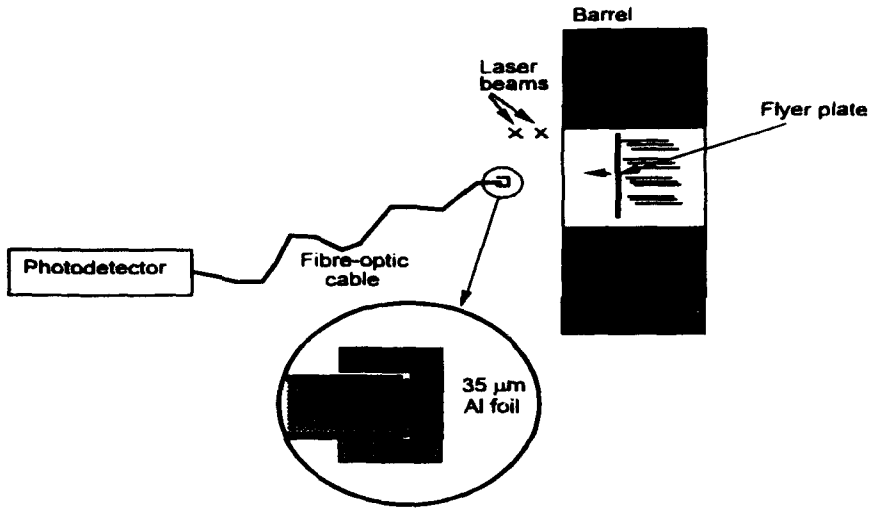

Figure 11: The front-on fibre optic impact arrangement. The placement of the front of the optic fibre and the second laser beam was such that the two were co-linear.

Two different photodetector circuits were used during the break-beam tests. The first is shown in Figure 12. The second circuit [12] (Fig.13) has a faster response and was needed to resolve the beam breaks for the second laser break-beam arrangement.

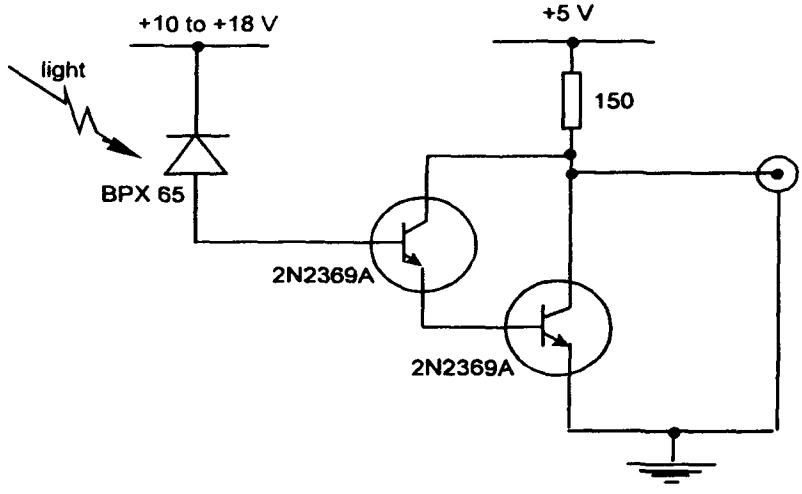

Figure 12: Photodetector circuit No.1.

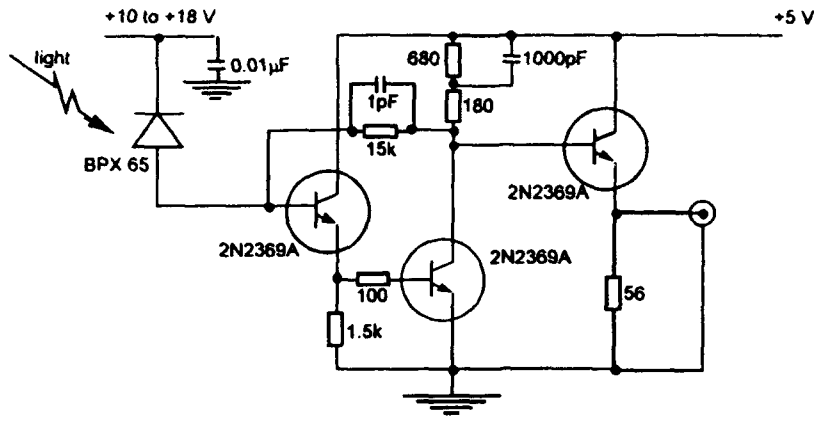

Figure 13: Photodetector circuit No.2.

2.3.3 *Particle, Shock,and Free-Surface Velocity*

The techniques used for particle, shock, and free-surface velocity measurements were limited to optical techniques (interferometry and fibre-optic).

For two transparent materials (Lexan and Perspex), the VISAR was used to measure the flyer velocity up to the moment of impact with the target. The shock velocity was calculated from its measured transit time through the target (Fig.14). The transit time was determined from the intensity variations of the reflected laser light detected by the PMTs in the VISAR. The particle velocity was assumed to be one-half of the flyer velocity. Target thicknesses of no greater than 4 mm were used to ensure that only the unattenuated shock velocity was measured (i.e., a target was not thick enough for the shock velocity to have been reduced by lateral release waves or the rarefaction wave from the flyer's free-surface).

For aluminium alloy 3105 targets, the VISAR was configured for measurement of the free-surface velocity of the back surface (Fig.15) by reinstalling the beam reducing telescope and using a 50 mm focal length lens to focus the laser beam on to the target. The targets were impacted by 0.47 mm thick Lexan flyers. The nominal firing voltage was 5 kV and the flyer launch position to target distances used were 12 mm and 25 mm. The flyer and shock velocities were not measured.

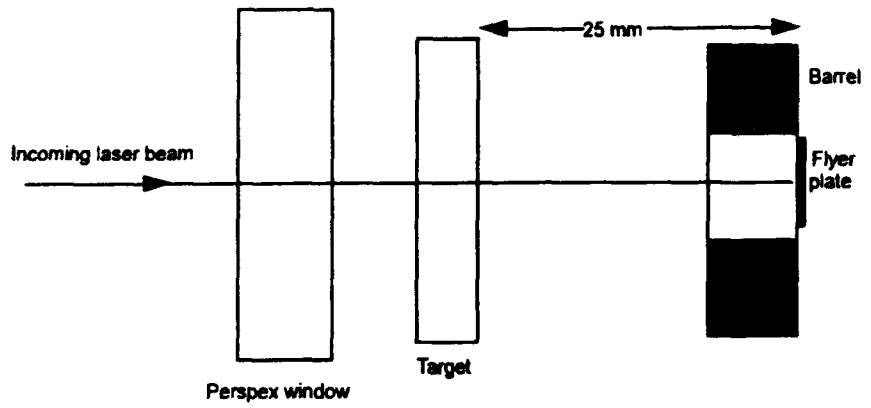

Figure 14: The pre-shot arrangement for the impact experiments with the plastic targets.

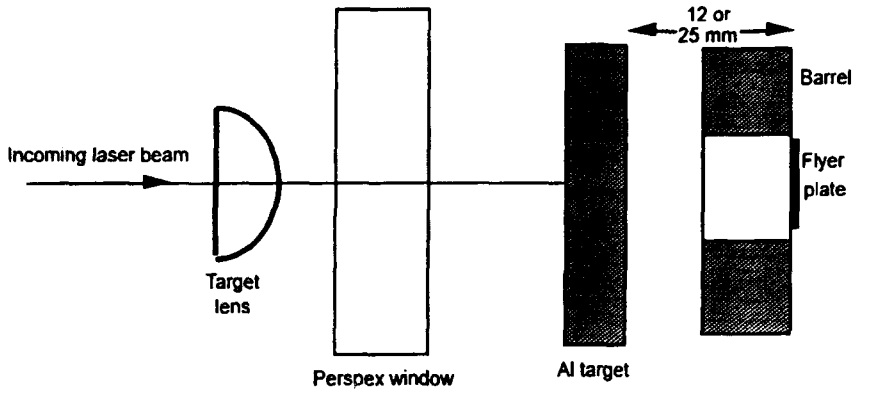

Figure 15: The pre-shot arrangement for the impact experiments with aluminium alloy 3105.

In some tests, a He-Ne laser beam was directed at the transparent targets (Fig.16). The reflections from the target surfaces were collected by a fibre-optic coupler for fibre-optic carriage to a photodetector. In this arrangement the shock transit time was to be determined from detector pulses expected to occur at times corresponding to loss of reflectivity of the target surfaces due to flyer impact and free-surface motion.

A typical instrumentation arrangement used for the above tests is shown in Figure 17.

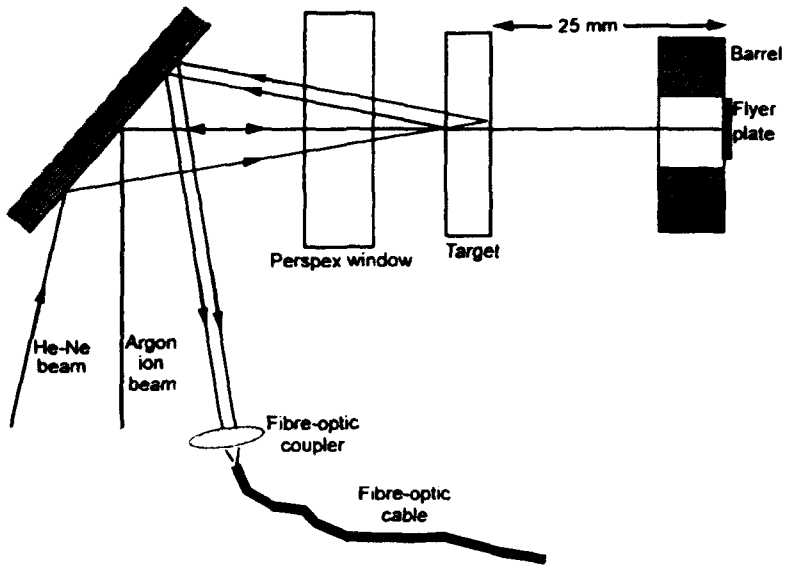

Figure 16: Arrangement with laser beam for shock transit time measurement.

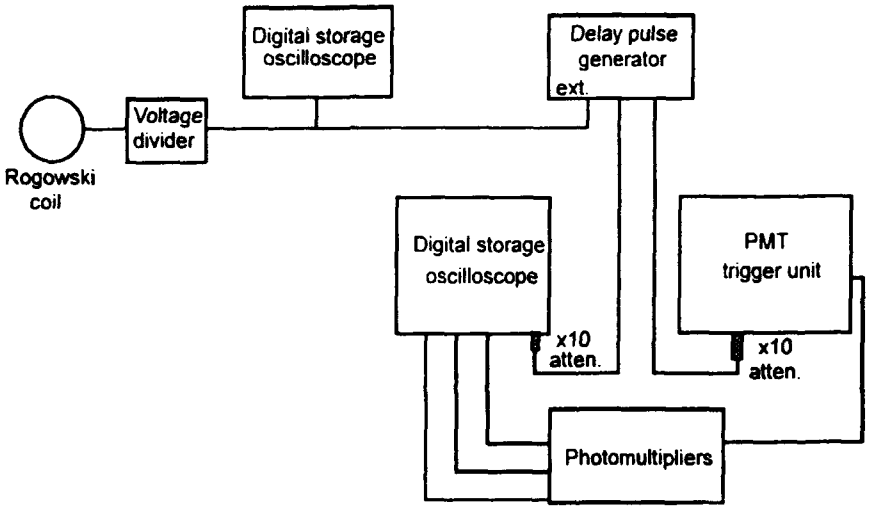

Figure 17: Block digram of the instrumentation arrangement for the impact experiments.

2.4 *High-Speed Photography*

High-speed photography was used to show the material or phenomenon being sensed by the laser break-beam velocity measurement arrangement. Of initial interest was the air shock ahead of the flyer. To improve its visibility, the air shock was photographed against a background of alternate black and white lines on a flat screen (Fig.18). The screen was positioned parallel to, and about 25 mm from, the line of flight of the flyer. Illumination of the screen was by means of

self-light from the bridge burst. The image converter camera, Imacon 790, was fitted with a 80-240 mm zoom lens and a No.2 neutral-density filter. The camera was configured to produce 8 frames at a framing rate of 2×10^6 frames/s. The camera was triggered via a delay pulse generator which in turn was triggered via the Rogowski coil signal. The nominal firing voltage for all tests was 5 kV. Some tests were performed with barrel diameters of 7 mm instead of 11.5 mm.

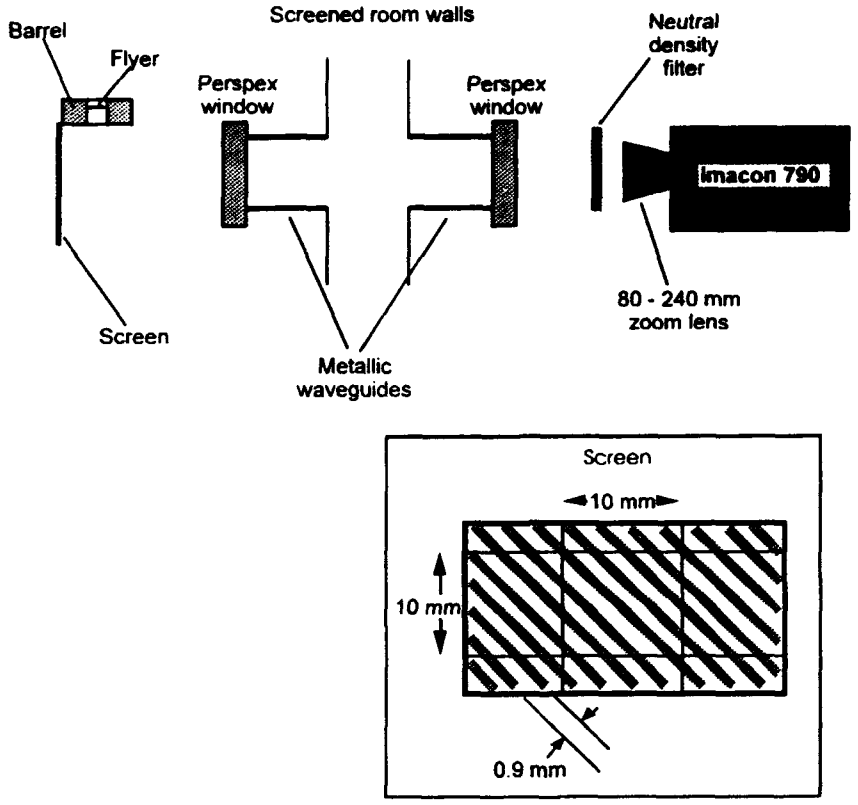

Figure 18: Schematic diagram of the arrangement used for high-speed photography of the flyer.

3. *Results and Discussion*

3.1 Calibration Curves

A typical velocity-time record, along with the Lissajous figure from which it was calculated, is shown in Figure 19. The peak flyer velocities obtained from these records are shown plotted against firing voltages in the calibration curves of Figure 20.

The initial portion of the velocity-time record (Fig.19) has several steps corresponding to shock reverberations in the flyer [13]. Apart from these steps, the flyer acceleration is smooth indicating that the tamper/bridge foil bond is sound [14]. The velocity steps occurred for both the 15 μm and 35 μm thick bridge foils. The steps possibly indicate that the bridge foils were too thin [14]. A suggested range for the ratio of flyer thickness to bridge foil thickeness is 5:1 to 10:1 [15]. This indicates that higher velocities might have been obtained if the bridge foil thickness was in the range 50 to 100 μm. The significant difference in performance between the 15 μm and 35 μm thick bridge foils can presumably be explained on this basis. Model calculations [4] have indicated that a bridge foil thickness in the range 75 to 100 μm should be used. However, subsequent tests [4] with 120 μm thick foils seemed to produce residual aluminium and the flyer performance was considered not significantly different to that for 25 μm foils (the velocity measurements were performed with a break-wire technique). One limit to the range of bridge foil thickness would be skin depth. Using the ringdown frequency of 28 kHz for the electric gun, the skin depth was calculated to be about 500 μm and therefore bridge foil thickness up to 100 μm are not expected to be a problem.

The current signal in Figure 21 shows that the bridge burst occurs about 4 μs after the initial current rise. Taking the 9 μs quarter-period of the ringdown as a guide, the bridge burst therefore occurs well before the current peak. The current rises again after burst and some acceleration due to a Lorentz force could be expected [14]. The increase in flyer velocity (Fig.19) following the initial acceleration is presumably due to this effect.

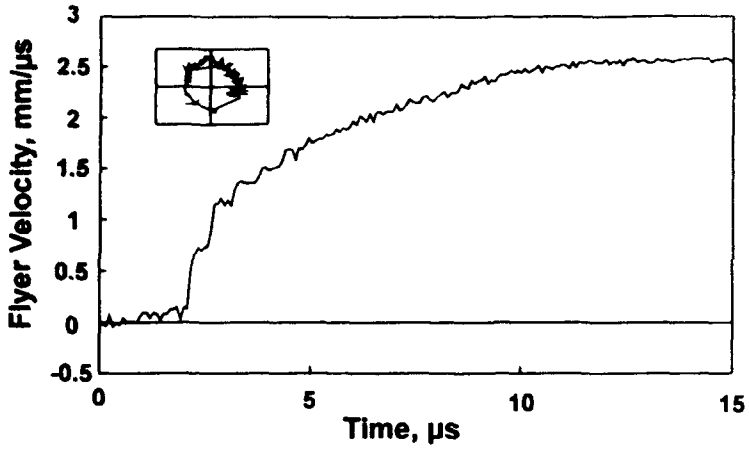

Figure 19: Typical velocity-time record and Lissajous figure (inset).

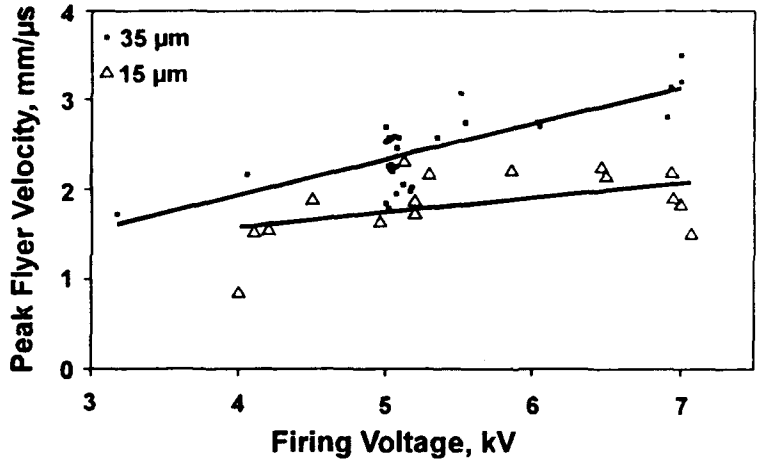

Figure 20: Peak flyer velocity versus firing voltage calibration curves for the 15 µm and 35 µm thick bridge foils.

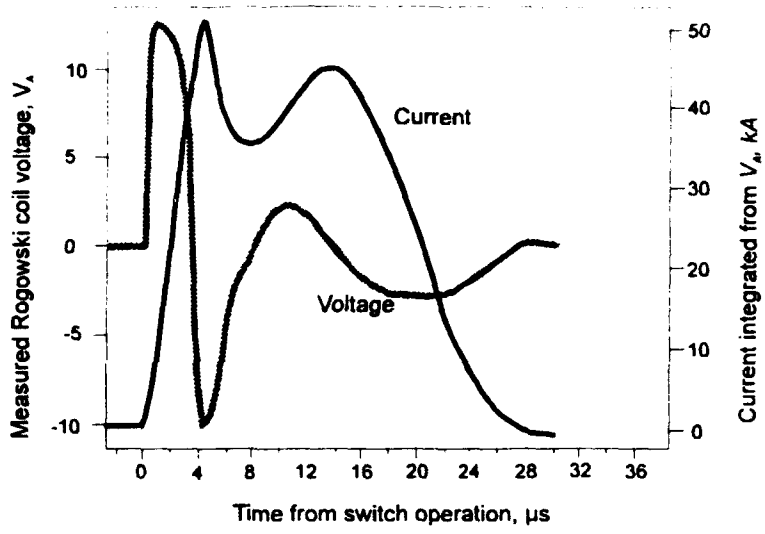

Figure 21: Bridge foil current-time history obtained from integration of Rogowski coil signal.

Many of the firings did not produce valid flyer velocity data. Some data were deemed unusable because the VISAR signals were too high (clipped) or low (noisy), or because the signals were lost before the flyer had reached its peak velocity (see Section 3.2). For other firings, no flyer velocity data were obtained; typically, this was because of triggering faults. The most frequent triggering fault was due to vagaries of the micro-switch/pneumatic pull-switch assembly. Many of the data for the 35 μm thick bridge foils were from the impact experiments where the firing voltage was about 5 kV.

In impact experiments where the particle velocity is derived from the flyer velocity but the flyer velocity cannot be measured by the VISAR or some other suitable means, the calibration curves could be used [2]. However, for a given firing voltage, the predicted peak flyer velocity calculated using the calibration curve for the 35 μm bridge foil (Fig.20) would have an uncertainty (3σ) of greater than ± 0.7 mm/μs. For a low flyer velocity (1.5 mm/μs) this corresponds to an uncertainty greater than ± 45%.

To obtain Hugoniot data to an accuracy better than ± 10% requires velocity uncertainties of less than ± 0.1 mm/μs. Clearly, the velocity versus firing voltage calibration curves are unsuitable. The reason for the lack of repeatability of the electric gun was not investigated.

An alternative method for obtaining the flyer velocity during impact experiments is to measure the flyer transit time from the launch position to the impact position and then calculate the velocity from a peak flyer velocity versus transit time calibration curve. The data for the curve is obtained by integrating the velocity-time records mentioned above to obtain distance-time records. Then, for a given flyer/target stand-off distance, the transit time is extracted from these records. In this way, for the 35 μm bridge foil and a flyer/target stand-off distance of 25 mm, the peak flyer velocity versus transit time curve shown in

Figure 22 was obtained. The uncertainty (3σ) for a predicted velocity using this curve is about ± 0.3 mm/μs.

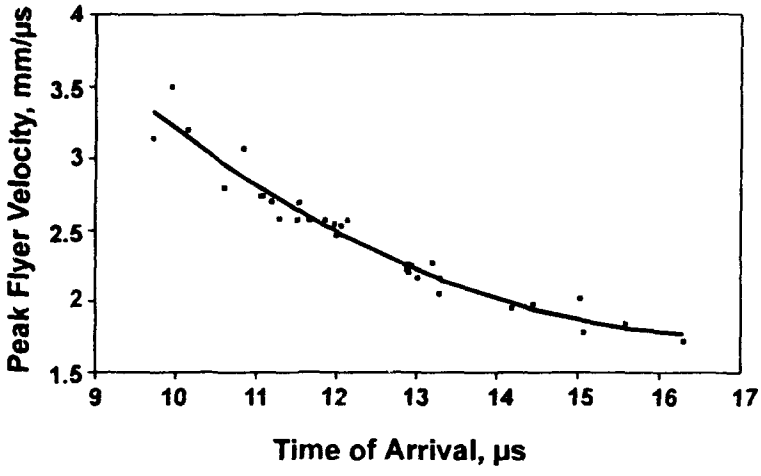

Figure 22: Peak flyer velocity versus time of arrival calibration curve for a bridge foil thickness of 35 μm and flyer/target stand-off distance of 25 mm.

3.2 *Laser Break-Beam*

Average velocities obtained from the single and double laser break-beam velocity measurement systems are shown in Figure 23. Included are average values calculated from distance-time curves obtained by integration of VISAR velocity-time curves and two average values obtained from the TOA system.

The single break-beam velocities are slightly higher than the VISAR average values. The TOA values are in close agreement with the VISAR values. However, the double break-beam velocities are less reproducible than the single break-beam data and sometimes 50% greater than the VISAR calibration curve. These higher velocities are similar to those obtained using an infinite barrel (i.e., no barrel) where the average velocity was measured by means of a break-wire technique [4]. In the present work, three tests were performed with no barrels and a firing voltage range of 5.0 to 5.05 kV for comparison with eleven of the 11.5 mm diameter barrel tests that occured in the same firing voltage range. The mean peak flyer velocities were 2.06 mm/μs (σ = ± 0.03 mm/μs) and 2.32 mm/μs (σ = ± 0.3 mm/μs), respectively. The performance of the gun is improved by about 11% when using the 11.5 mm diameter barrel.

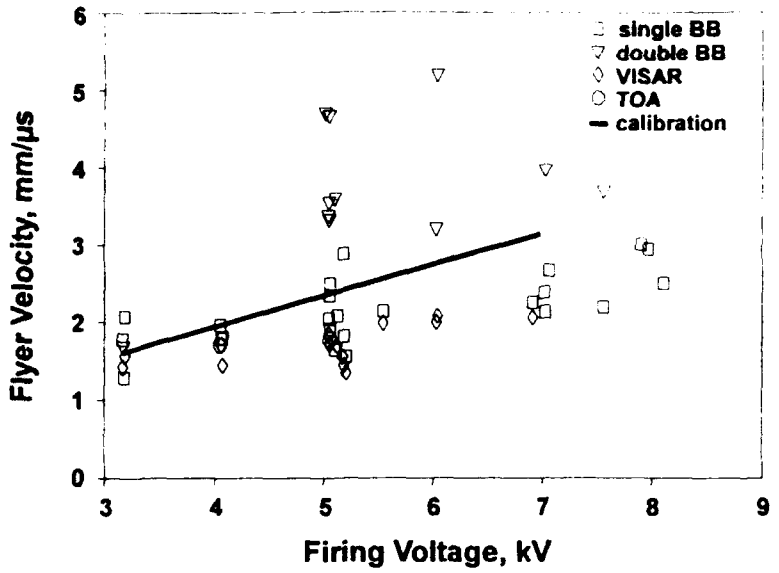

Figure 23: Comparison of peak flyer velocity calibration curve with average velocities obtained from the laser break-beam, TOA, and VISAR measurement systems.

The high-speed photographs revealed that the beams in the double break-beam velocity system were probably being triggered by plasma exiting from the barrel ahead of the flyer (Fig.24), which would explain the high velocities otained with this system. The plasma is considered also to be the cause of the loss of VISAR signals for some shots before the flyer had reached its peak velocity. The leakage of plasma past the flyer, which would presumably occur in a variable way from shot to shot, may also affect the flatness and tilt of the flyer and contribute to the lack of repeatability of the electric gun.

The closeness of the average velocities for the single break-beam system to the VISAR average velocities suggests that the plasma is retained by the flyer until the flyer is near the barrel exit. Around barrel exit the plasma jets past the flyer thereby producing the apparently high flyer velocities. The single break-beam values are more consistent than the double break-beam values which also suggests that plasma effects are not present, at least until near barrel exit.

It was considered that the propensity for the plasma to exit from the barrel ahead of the flyer was due to the barrel diameter (11.5 mm) being slightly larger than the bridge width (10 mm). To investigate this, several high-speed photographs were taken using 7 mm diameter barrels. A significant decrease in plasma leakage past the flyer occurred (Fig.25).

3.3 *Impact*

In general, for the transparent targets, the PMT signals showed a rapid increase in light intensity at impact corresponding to light emission from the compression of air between the flyer and target [16]. The signals then fell rapidly to a very low

level, followed by a rapid increase again when the shock reached a surface/air interface (Fig.26). For a laminated target with a small air space at the internal interface, when the shock arrived at the interface the signals rapidly increased and then rapidly fell back to a low level.

The compression of the air prevents the clear definition of impact time. In addition, the sharpness of the intensity changes at both the front and back surfaces sometimes would have been affected by non-planar flyer impact (the flatness and tilt of any one flyer at impact was unknown but the high-speed photographs show that sometimes the flyers are curved and the tilt appreciable).

Thus it was not possible to obtain accurate shock transit times in the target from the PMT signals. This is reflected in the vertical 'error bars' shown in the shock velocity versus particle velocity plots of Figures 27 and 28 for Lexan and Perspex, respectively. Each bar is the difference in shock velocity calculated using transit times t_1 and t_2 (Fig. 26). The shock velocity was taken to be mid-way between the two values.

The method could be expected to be improved by performing the tests at low air pressures, thereby eliminating the light emission prior to impact. The pressure pulse from the compressed air would also be eliminated, though this is probably not a problem because it attenuates rapidly in the target [16]. However, even if this was done, the accuracy of the shock velocity measurement would still have a systematic error because the flyer comprises two different layers. The presence of the retroreflective layer means that the shock velocity attributable to the primary layer is not reached until some finite distance into the target (Fig. 29). The magnitude of the error depends firstly on the shock impedance mismatch of the two layers and secondly on the relative target, retroreflective, and primary layer thicknesses.

Reduction of this error requires the use of a much thinner retroreflective or reflective layer. Several tests were performed with thin aluminium foil bonded to the primary layer instead of the retroreflector. The reflectivity of the two foil surfaces as received were different (specular and matt) but it was found either could be used. Hugoniot data obtained using 0.47 mm thick Lexan flyers with 35 μm thick aluminium foil on the front surface are shown in Figure 30. Half of the data were obtained for targets 16 mm from the barrel muzzle; for the other half the targets were about 1 mm from the muzzle. Further, four of the six data points were obtained using a smaller barrel diameter, viz. 9 mm. No consistent trends were found to show the effects of using the different target stand-off distances and barrel diameters. Moreover, there is no marked improvement in the quality of the data obtained with the thin aluminium layer compared to the thicker retroreflective layer.

The accuracy of the published data shown in Figures 27, 28, and 30 is not readily available. From an alternative but less recent source [17], least squares linear fits (equation 1) to data for Perspex show standard deviations of ≈ 0.1 mm/μs for the shock velocity. For comparison, based on the limited range of data obtained, the experimental techniques used in the present work could be expected to produce standard deviations of the order of 0.5 mm/μs.

Measurement of shock transit times using the laser beam arrangement (Fig.16) was unsuccessful because the laser signals were obscured by very much stronger light signals from the self-luminious plasma.

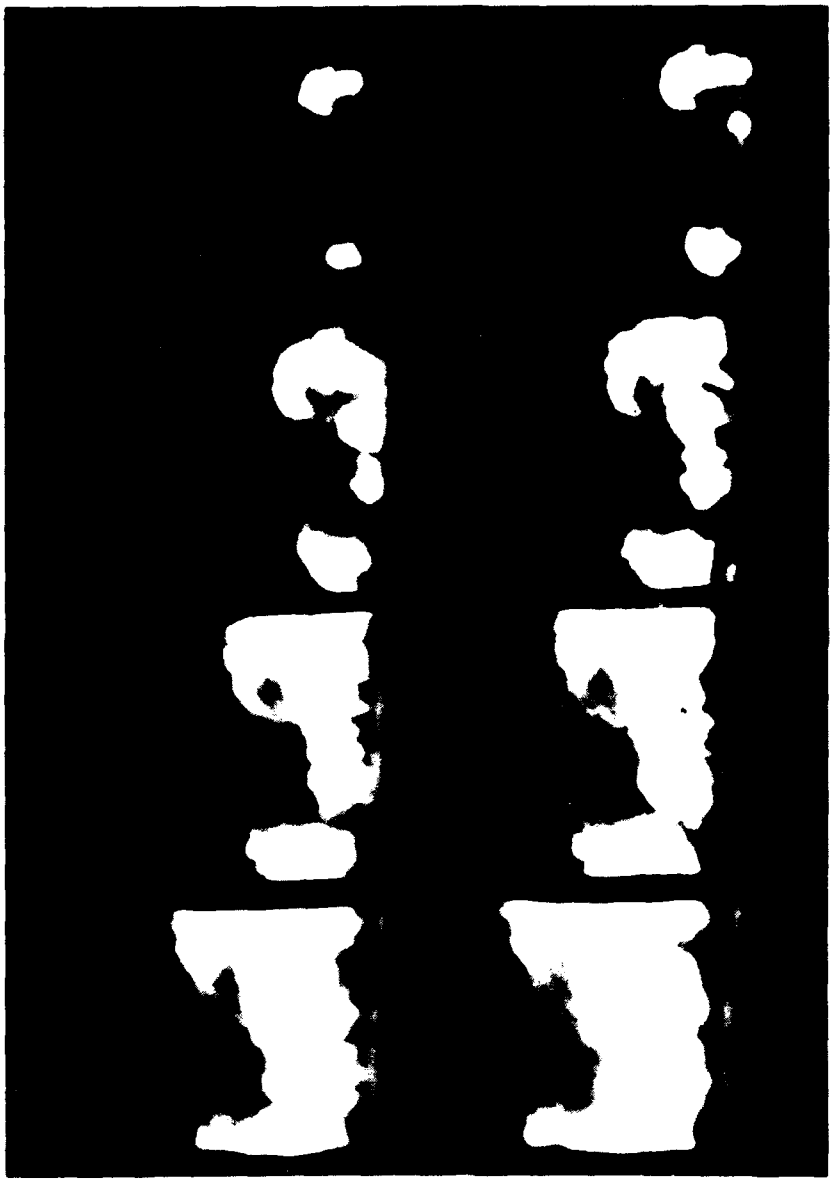

Figure 24: High-speed photograph of plasma and flyer exiting from a 11.5 mm diameter barrel.

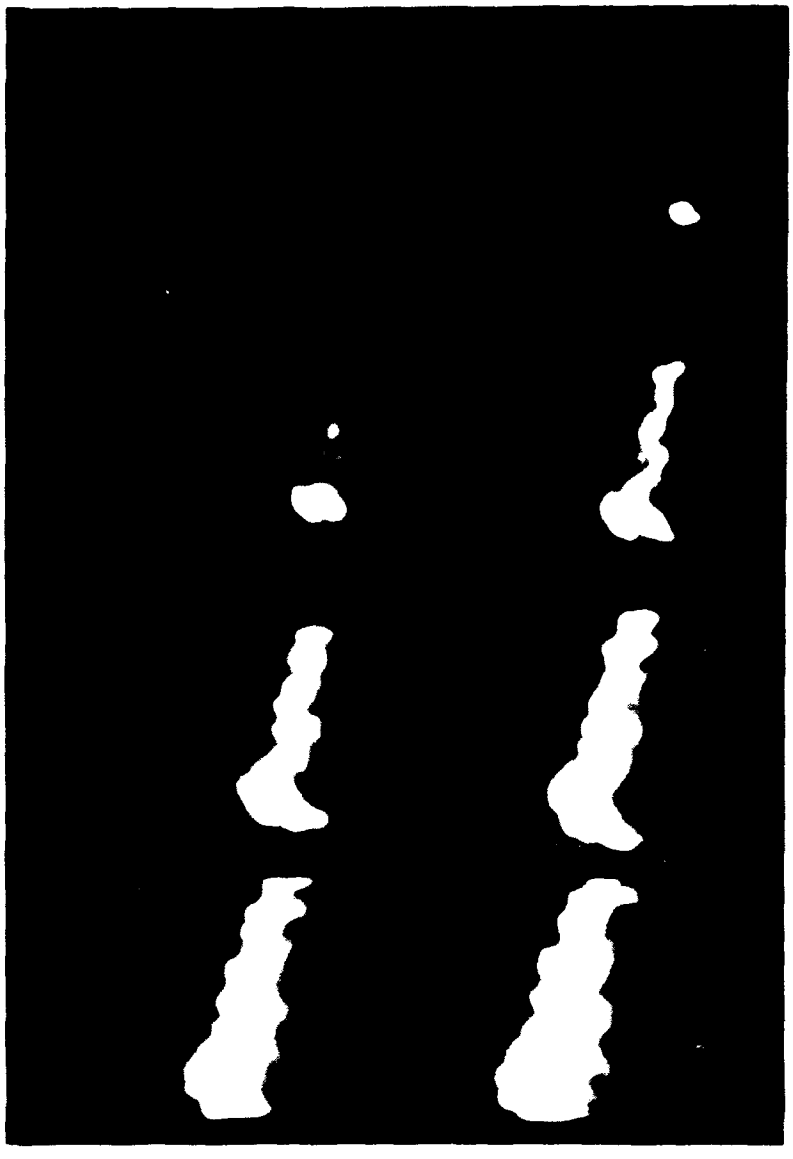

Figure 25: High-speed photograph of plasma and flyer exiting from a 7 mm diameter barrel.

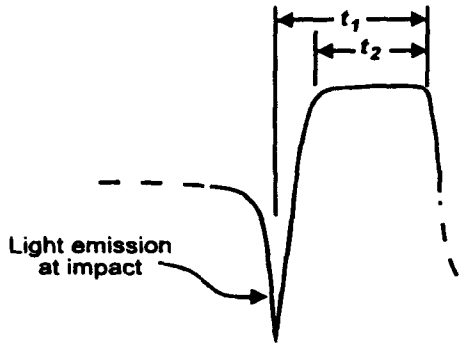

Figure 26: Schematic diagram of the portion of a PMT signal used for the determination of shock velocity

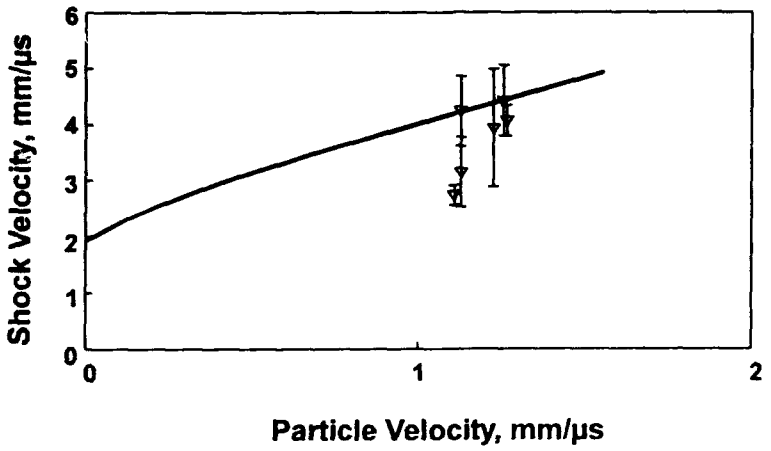

Figure 27: Hugoniot measurements for Lexan from impact experiments using a laminated flyer (retroreflector on Lexan). The solid line is from published data [6].

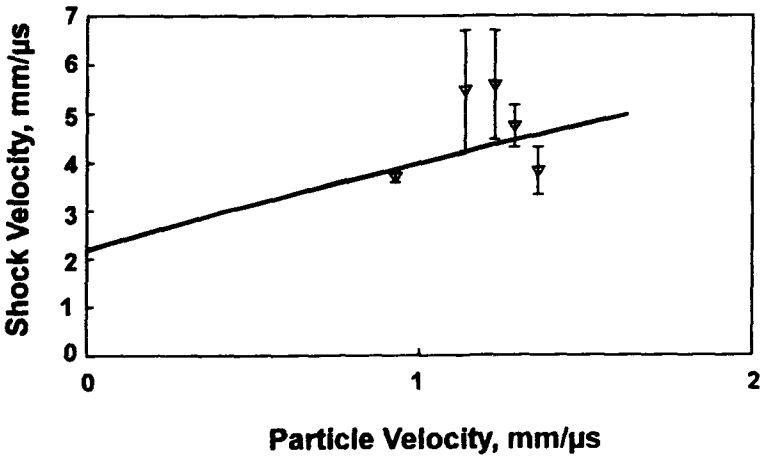

Figure 28: Hugoniot measurements for Perspex from impact experiments using a laminated flyer (retroreflector on Lexan). The solid line is from published data [6].

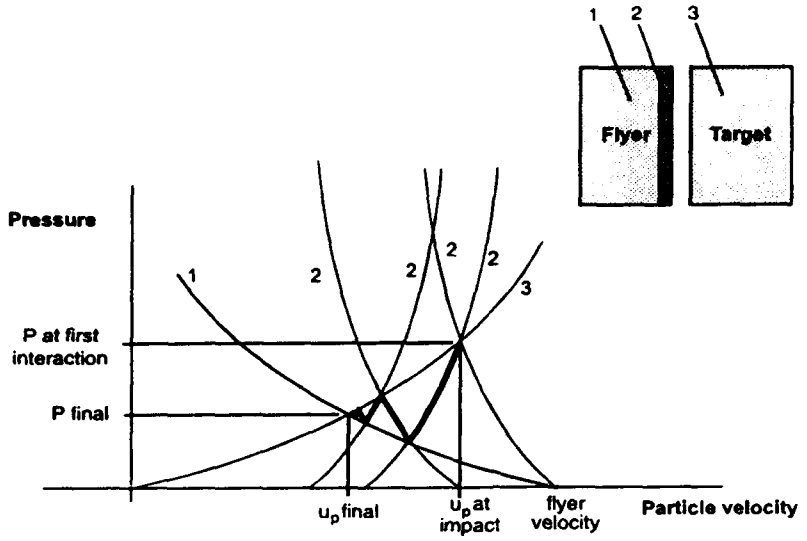

Figure 29: Schematic diagram of the shock reverberations which occur with a laminated flyer. In this diagram the shock impedance of the facing material (2) is very much greater than that of the backing (1). In addition, the target (3) and the backing are of the same material. With a thin facing material, such as the aluminium foil of 35 μm thickness, the shock velocity in the target will rapidly approach the same value that would be obtained if the facing material thickness was zero.

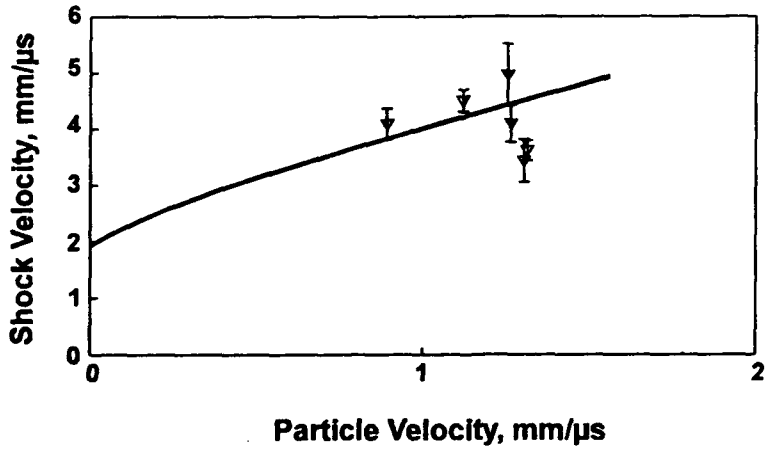

Figure 30: Hugoniot measurements for Lexan from impact experiments using a Lexan flyer with a thin facing material (35 μm thick aluminium foil). The solid line is from published data [6].

In the tests with the aluminium alloy 3105 targets, the flyer velocity could not be measured either by means of the VISAR or the TOA calibration curve (since the flyer did not include the retroreflector). However, assuming that the flyer velocity was about 2.5 mm/μs, the calculated free-surface velocity, U_{fs}, is ≈ 1.4 mm/μs. The Hugoniots used in this calculation, for Lexan and aluminium alloy respectively, were

$$U_s = 2.12 + 1.86 u_p \quad (5)$$

$$U_s = 5.3 + 1.35 u_p \quad (6)$$

The Lexan Hugoniot is a least squares fit to published data [6]. The Hugoniot for the aluminium alloy is a representative one based on published data for some other aluminium alloys (1100, 2024, and 6061) [6]. The back surface of the targets spalled, producing a velocity-time history of the form shown in Figure 31. The free-surface velocity was based on the assumption, due to the finite response time (≈ 5 ns) of the VISAR PMTs , that one fringe was lost [18]. The amplitude drop from the peak to the first minimum gave the velocity change, Δu (Fig.31). This enabled the spall strength, σ_S , to be calculated using [19]

$$\sigma_s = \frac{1}{2} \rho_o U_s \Delta u \quad (7)$$

where ρ_o = initial density of the aluminium alloy, and U_S = shock velocity in the aluminium alloy. The results are shown in Table 1. Spall strength data for aluminium alloy 3105 could not be found in the literature. Spall strength values for various aluminium alloys typically are in the range 1 to 2 GPa [20].

4. Conclusions

The MRL large-scale electric gun was calibrated successfully using a VISAR velocity interferometer. Two different exploding bridge foil thicknesses were used, viz. 15 μm and 35 μm. In both cases, the flyers were approximately 10 mm in diameter but with 35 μm thick foils the gun produced higher peak flyer velocities; these were in the range 1.7 to 3.5 mm/μs for a corresponding firing voltage range of 3.2-7.0 kV.

The gun was found to have low repeatability. Thus, with 35 μm thick foils, the uncertainty for a prediction made using the peak flyer velocity versus firing voltage calibration curve would be greater than ± 0.7 mm/μs. However, it was shown that by manipulation of the data, a peak flyer velocity versus time of arrival (at 25 mm) calibration curve could be obtained which would reduce the uncertainty by a factor of about two.

Laser break-beam methods for measuring flyer velocity, particularly the double beam variant, consistently produced high velocities and thus were found to be unreliable. From high-speed photographs, it was inferred that this was due to leakage of plasma past the flyer. This leakage may have been exacerbated by the use of a barrel that was slightly larger than the bridge foil.

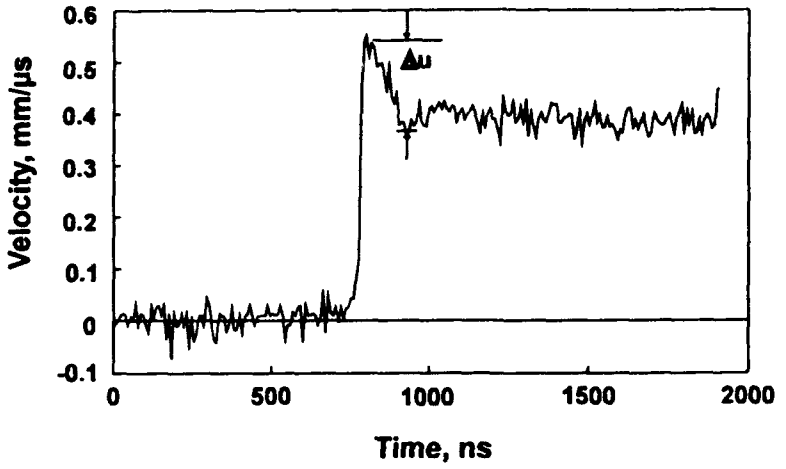

Figure 31: Velocity-time record for aluminium alloy 3105 target with spalling of the front surface.

Table 1: Aluminium Alloy 3105 Targets - Spall Strength Results

Calculated U_{fs} (mm/μs)	Measured U_{fs} (mm/μs)	Measured Spall Strength (GPa)
	1.38	1.33
	1.50	1.32
1.4	1.27	2.13[a]
	1.44	1.54

a. Data dubious as spallation occurred off-centre from the axis of the laser spot.

Shock and particle velocity data were obtained for transparent materials only. Data obtained for Perspex (PMMA) and Lexan (polycarbonate) from impact experiments were in general agreement with the known Hugoniots for these materials. The quality of the data could have been affected by the laminated form of the flyers (Lexan and retroreflective tape). This form was used to facilitate calibration. It was subsequently found that Lexan flyers with a thin layer of aluminium could be used instead. Impact experiments with these gave no marked improvement.

The opaque material tested was aluminium alloy 3105 for which only spall strength data were obtained. These data were also in general agreement with the known spall strength for various aluminium alloys.

This work has shown that the electric gun has the potential to be useful for obtaining shock Hugoniot and spall strength data for materials but in its present form the Hugoniot data would be imprecise. The gun performance and measurement techniques are not yet optimal. Different barrel diameters and bridge foil thicknesses may produce a more consistent and improved performance. Tests need to be performed with the gun surrounded by a low pressure environment. Other methods for measuring shock velocity may be needed and the planarity of the flyers may need to be studied further.

5. *Acknowledgements*

The specification and acquisition of the Safety Interlock System was co-ordinated by Dr M.Podlesak. One of the photodetector circuits was based on one kindly provided by Mr P.Collins. The high-speed photography was conducted in collaboration with Mr T.Kinsey. Discussions with Dr D.D.Richardson were greatly appreciated.

6. *References*

1. Stilp, A. J. and Hohler, V. (1990).
Experimental methods for terminal ballistics and impact physics. In: *High Velocity Impact Dynamics.* (J. A. Zukas, ed.). Wiley, NY.

2. Gathers, G. R., Chau, H. H., Osher, J. E., and Weingart, R. C. (1990).
Hugoniot measurements with the LLNL electric gun facility. In: *Shock Compression of Condensed Matter-1989.* (S.C.Schmidt, J.N.Johnson, and L.W.Davison, eds.). Elsevier Science Publishers.

3. Walker, F. E. and Walsey, R. J. (1969).
Critical energy for shock initiation of hetergeneous explosives. *Explosivstoffe,* 17, 9.

4. Podlesak, M., Richardson, D. D., and Olsson, C. (1992).
An exploding foil flying plate generator for shock wave studies— calibrations. (MRL Research Report MRL-RR-1-92). Maribyrnong, Vic.: Materials Research Laboratory.

5. Hatt, D. J. (1991).
A VISAR velocity interferometer system at MRL for slapper detonator and shockwave studies. (MRL Technical Report MRL-TR-91-42). Maribyrnong, Vic.: Materials Research Laboratory.

6. Steinberg, D. J. (1991).
Equation of state and strength properties of selected materials. (LLNL UCRL-MA-106439). Livermore, CA: Lawrence Livermore National Laboratory.

7. Ternan, J. G. (1991). *Safety of electro-explosive devices near the EBF flyer facility.* (Unpublished work). Maribyrnong, Vic.: Materials Research Laboratory.

8. Lindgren, E. A. (1975).
Demountable RF shielded enclosures. In: *1975 International Symposium on Electromagnetic Compatibility* .

9. Mardiguian, M. (1988).
*Grounding and bonding— A handbook series on electromagnetic interference and compatibility, Vol.*2. Interference Control Technologies, Inc.

10. Beck, E. (1954).
Lightning protection for electric systems. McGraw-Hill Book Company.

11. Terman, F. E. and Pettit, J. M. (1952).
Electronic measurements. McGraw-Hill Book Company.

12. High speed fiber optic link design with discrete components.
Hewlett Packard Application Note 1022.

13. Osher, J. E., Chau, H. H., Gathers, G. R., and Weingart, R. C. (1990).
Characteristics of flyer impact for one-dimensional shock-wave study applications. In: *Shock Compression of Condensed Matter-1989.* (S.C.Schmidt, J.N.Johnson, and L.W.Davison, eds.). Elsevier Science Publishers.

14. Chau, H. H. and Osher, J. E. (1990).
Application of Fabry-Perot velocimetry to hypervelocity impact experiments. In: *SPIE Vol. 1346— Ultrahigh- and High-Speed Photography, Videography, Photonics, and Velocitmetry '90.* (L.L. Shaw, P.A. Jaanimagi, B.T. Neyer, eds.).

15. McDaniel, O. K. (1990).
Exploding foil initiators—an overview. In: *Proceedings of the Fourteenth Symposium on Explosives and Pyrotechnics.*

16. Harlan, J. G., Rice, J. K., and Rogers, J. W. (1981).
The role of air and other gases in flyer plate initiation of explosives. In: *Proceedings of the Seventh Symposium (International) on Detonation.*

17. van Thiel, M. (1977). *Compendium of Shock Wave Data.* (LLNL UCRL-50108-Vol.3). Livermore, CA: Lawrence Livermore National Laboratory.

18. Erskine, D. J., Green, L., and Tarver, C. (1990).
VISAR wave profile measurements in supra-compressed HE. In: *Shock Compression of Condensed Matter-1989.* (S.C.Schmidt, J.N.Johnson, and L.W.Davison, eds.). Elsevier Science Publishers.

19. Froeschner, K. E., Maiden, D. E., and Chau, H. H. (1989). Spall due to short high-intensity impulses. *J. Appl. Phys.* 65 (8)

20. Davison, L. and Graham, R. A. (1979). *Shock Compression of Solids.* Physics Reports, 55, No.4.

SECURITY CLASSIFICATION OF THIS PAGE **UNCLASSIFIED**

REPORT NO.	AR NO.	REPORT SECURITY CLASSIFICATION
MRL-TR-93-24	AR-008-293	Unclassified

TITLE

Calibration and testing of a large-scale electric gun for shock Hugoniot measurements

AUTHOR(S)
David J. Hatt and Philip F.X. Ryan

CORPORATE AUTHOR
DSTO Materials Research Laboratory
PO Box 50
Ascot Vale Victoria 3032

REPORT DATE	TASK NO.	SPONSOR
October, 1993	DST 92/293	DSTO

FILE NO.	REFERENCES	PAGES
G6/4/8-4441	20	37

CLASSIFICATION/LIMITATION REVIEW DATE

CLASSIFICATION/RELEASE AUTHORITY
Chief, Explosives Ordnance Division

SECONDARY DISTRIBUTION

Approved for public release

ANNOUNCEMENT

Announcement of this report is unlimited

KEYWORDS

Shock Hugoniot
Electric gun
VISAR
Exploding bridge foil
Spall strength

ABSTRACT

This report presents further work on the MRL large-scale electric gun facility including the use of a screened room and a purpose-built safety interlock system, calibration of an electric gun using a VISAR velocity interferometer, and tests on two laser break-beam arrangements for measuring flyer velocity. The VISAR was also used for making velocity measurements during some impact experiments on several materials to test the suitability of the facility for obtaining Hugoniot and spall strength data. The materials were Perspex and Lexan (polymethyl methacrylate and polycarbonate) and aluminium alloy 3105. The flyer velocities measured using the break-beam arrangements were compared with those measured by the VISAR. The agreement between the two methods was found to be poor and inconsistent. High-speed photographs show leakage of plasma past the flyer. Interruption of the laser beams by the plasma instead of the flyer seems to be the reason for the poor agreement. The Hugoniot and spall strength data were in general agreement with published data.

Calibration and Testing of a Large-Scale Electric Gun
for Shock Hugoniot Measurements

David J. Hatt and Philip F.X. Ryan

(MRL-TR-93-24)

DISTRIBUTION LIST

Director, MRL
Chief, Explosives Ordnance Division
Dr B.W. Thorpe
David J. Hatt
Philip F.X. Ryan
MRL Information Services

Chief Defence Scientist (for CDS, FASSP, ASSCM) — 1 copy only
Director (for Library), Aeronautical Research Laboratory
Head, Information Centre, Defence Intelligence Organisation
OIC Technical Reports Centre, Defence Central Library
Officer in Charge, Document Exchange Centre — 8 copies
Army Scientific Adviser, Russell Offices
Air Force Scientific Adviser, Russell Offices
Navy Scientific Adviser - data sheet only
Scientific Adviser, Defence Central
Director General Force Development (Land)
Senior Librarian, Main Library DSTOS
Librarian - MRL Sydney - data sheet only
Librarian, H Block
Serials Section (M List), Deakin University Library, Deakin University, Geelong 3217
NAPOC QWG Engineer NBCD c/- DENGRS-A, HQ Engineer Centre, Liverpool Military Area, NSW 2174
Librarian, Australian Defence Force Academy
Counsellor, Defence Science, Embassy of Australia - data sheet only
Counsellor, Defence Science, Australian High Commission - data sheet only
Scientific Adviser to DSTC Malaysia, c/- Defence Adviser - data sheet only
Scientific Adviser to MRDC Thailand, c/- Defence Attache - data sheet only
Head of Staff, British Defence Research and Supply Staff (Australia)
NASA Senior Scientific Representative in Australia
INSPEC: Acquisitions Section Institution of Electrical Engineers
Head Librarian, Australian Nuclear Science and Technology Organisation
Senior Librarian, Hargrave Library, Monash University
Library - Exchange Desk, National Institute of Standards and Technology, US
Exchange Section, British Library Document Supply Centre
Periodicals Recording Section, Science Reference and Information Service, UK
Library, Chemical Abstracts Reference Service
Engineering Societies Library, US
Documents Librarian, The Center for Research Libraries, US